ENGINEERING RESEARCH INSTITUTE
UNIVERSITY OF MICHIGAN
ANN ARBOR

SMALL SIGNAL HETERODYNE MIXERS WITH EXCESSIVE INJECTION AMPLITUDES

Technical Report No. 62
Electronic Defense Group
Department of Electrical Engineering

By: J. F. Cline

Approved by: ______________
J. A. Boyd

Project 2262

TASK ORDER NO. EDG-8
CONTRACT NO. DA-36-039 sc-63203
SIGNAL CORPS, DEPARTMENT OF THE ARMY
DEPARTMENT OF ARMY PROJECT NO. 3-99-04-042

March, 1956

TABLE OF CONTENTS

LIST OF ILLUSTRATIONS

ABSTRACT

The theory of small-signal heterodyne mixers operating with very large injection potential swings is described. The mixer properties investigated are the conversion transconductance, the relative amplitudes of the difference-frequency and injection frequency components in the output, and the amplitude of the injection modulation-frequency component in the output in the case where the injection potential is amplitude-modulated to a small degree, as by power-supply ripple or noise, for example. The theoretical analysis is based upon two- and three-segment piecewise-linear approximations of the current and incremental transfer conductance curves, so that the mixer can be treated as a switch-type or commutator-type modulator. The method of constructing the approximations from the original curves is described. The result is a set of universal performance curves for all mixers of the particular class chosen to illustrate the method. The method can be extended to other classes of mixers.

SMALL SIGNAL HETERODYNE MIXERS WITH EXCESSIVE INJECTION AMPLITUDES

I. INTRODUCTION

This report describes the operation of small-signal heterodyne mixers in which the injection potential is a biased sinusoid which may be permitted to become much larger than in ordinary applications. Such excessive injection potentials are found either in applications where it is desired to obtain a decreasing conversion transconductance with an increasing injection potential or in applications where, for reasons independent of mixer performance considerations, it is either necessary or expedient to tolerate an excessive injection potential.

The term "small-signal" is used here to indicate a condition where the signal amplitude is too small to have an appreciable effect upon the value of the conversion transconductance. This condition is found in most superheterodyne receiver converters, analog multipliers, spectrum analyzers, etc. The mixer properties which are investigated here are the conversion transconductance, the relative amplitudes of the difference-frequency and injection-frequency components in the output, and the amplitude of the injection modulation-frequency component in the output in cases where the injection potential is amplitude-modulated to a small degree, as, for example, by noise or by power-supply ripple.

II. METHOD OF ANALYSIS

The method of analysis described here is illustrated by its application to a class of mixers having characteristic curves of the particular shape shown as solid lines in Fig. 1. The results can easily be extended to other classes of mixers. The essential properties of the solid curves in Fig. 1 are that the output current characteristic i has two horizontal sections at different levels while the incremental transfer conductance characteristic g has two horizontal sections both at zero level. Both curves are plotted with the instantaneous injection potential e_i as the abscissa. The details of the curved transitional sections which join the horizontal sections are unimportant.

It will be convenient in the discussion which follows to use the term "transitional potential range" in referring to the range of instantaneous injection potential e_i over which the transitional curved sections of i and g extend. In most mixer applications the swing of the injection potential is usually not much larger than, if as large as, the transitional potential range. This is true in many superheterodyne radio receivers, for example. A discussion of the conversion transconductance of small-signal heterodyne mixers which are operating with injection potential swings of the magnitude often employed in superheterodyne receivers has been given by Herold[1], and can be found in popular textbooks.[2,3]

1. Herold, "The Operation of Frequency Converters and Mixers for Superheterodyne Reception," Proc. I.R.E., Vol. 30, February, 1942, p. 8.
2. Seely, "Electron Tube Circuits," McGraw-Hill, 1950, pp. 359-61.
3. Van Voorhis, "Microwave Receivers," McGraw-Hill, 1948, pp. 138-48.

2262 A-68-68 BM 10-28-55

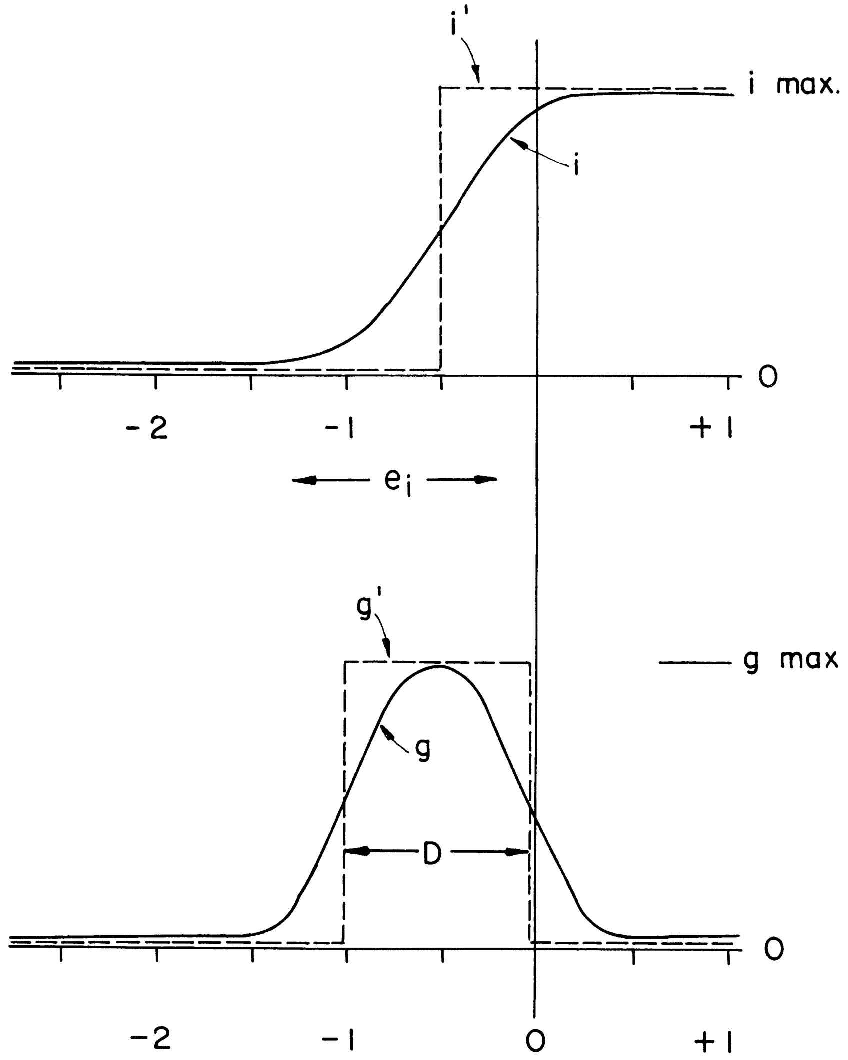

FIG. I. OUTPUT CURRENT (i OR i') AND INCREMENTAL TRANSFER CONDUCTANCE (g OR g') AS FUNCTIONS OF THE INSTANTANEOUS TOTAL INJECTION POTENTIAL e_i. THE DASHED CURVES i' AND g' ARE THE PIECEWISE-LINEAR APPROXIMATIONS.

When the injection potential swing is not large in comparison with the transitional potential range, the details of the curve shape are quite important in the quantitative analysis. Herold's analysis, for example, uses several points on the transitional part of the curve in order to take adequate account of the details of the shape. On the other hand, when the injection potential swing is very large in comparison with the transitional potential range, the fine details of the curved section are found to be relatively unimportant in the quantitative analysis. This makes it possible to replace the solid curves in Fig. 1 with the piecewise-linear curves i' and g', which are drawn as dashed lines in the same figure. The mixer then becomes essentially a switch-type or commutator-type modulator, which has been discussed by Caruthers[4] and by Peterson and Hussey.[5] For any particular mixer, the curves corresponding to the solid lines of Fig. 1 are obtained experimentally and it is difficult in general to obtain suitable mathematical expressions for them. The piecewise-linear curves, on the other hand, are easily described in mathematical terms. The problem is to find a way of constructing the piecewise-linear curves so that when they are analyzed mathematically, the results will be, as nearly as possible, the same as the results obtained from the solid curves.

Consider a mixer in which there is a resistive load R_L and an applied signal potential of instantaneous value e_s. The incremental transfer conductance g is then defined as the partial derivative of the instantaneous load current i with respect to e_s. A distinction must sometimes be made between this incremental transfer conductance g of the circuit as a whole and the ordinary incremental

4. Caruthers, "Copper Oxide Modulators in Carrier Systems," B.S.T.J., Vol. 18, pp. 315-337, April, 1939.

5. Peterson and Hussey, "Equivalent Modulator Circuits," B.S.T.J., Vol. 18, pp. 32- 37, Jan. 1939.

transconductance g_m of the mixer tube alone. The distinction is not necessary when R_L is so small as to have no appreciable effect upon i, but when g and g_m do differ appreciably, they are often approximately proportional to each other for different values of the instantaneous injection potential e_i, so that when relative rather than absolute values are being considered, g and g_m may often be considered the same.

The above definition of g applies to both single-input and double-input mixers. In a single-input mixer, e_s and e_i are applied in series to the same input terminal-pair, so that g is equal to the partial derivative of i with respect to either e_s or e_i. In a double-input mixer, however, e_s and e_i are applied to separate terminal-pairs and in general they have unequal effects upon i. Therefore g is not equal to the partial derivative of i with respect to e_i in a double-input mixer. Upon casual inspection of Fig. 1, it might be concluded from the shapes of the solid curves of i and g vs. e_i that a derivative relationship exists and that the solid curves of Fig. 1 therefore represent a single-input mixer. On the other hand, the piecewise-linear curves i' and g' certainly do not possess the derivative relationship. The analysis which follows is organized in such a way that a derivative relationship between the i' and g' curves is not required, and consequently the results may be applied to either single-input or double-input mixers.

In constructing the piecewise-linear curves, the discontinuities in g', which define the dynamic range D, are placed so that the area under g' is equal to the area under g and also so that the centers of gravity of the two areas are located at the same value of e_i. For convenience, the origin of the e_i scale is placed at the right-hand limit of D and the e_i scale units are chosen so that D equals unity. This serves to normalize the injection potential with respect to the dynamic range and thereby simplifies some of the mathematical expressions.

The discontinuity in i' is placed so that the area under i' is equal to the area under i, which results in most cases in placing the discontinuity somewhere near $e_i = -1/2$.

It will develop subsequently that the three mixer properties with which this paper is concerned can be expressed in terms of the zero- and first-order coefficients of i and g when they are expanded in Fourier series as functions of time. The reason for drawing the piecewise-linear curves with the equal area and center of gravity properties described above is that the zero- and first-order coefficients are approximately the same as those of the solid curves when this is done. The reason for this can be explained in terms of the g and g' curves as an example. Consider the transitional range of injection potential for which g has an appreciable value. This will be an interval of e_i somewhat larger than D, but much smaller than the total swing of the injection potential. If this swing extends quite far beyond both limits of the transitional range, time and potential will be quite linearly related within the range, and consequently the areas under g and g', which have been made equal to each other when these quantities are plotted against e_i, will now be approximately equal to each other when g and g' are plotted against time. Now let g and g' be expanded in Fourier series as functions of time, with the zero reference chosen so that they are even functions. If t is time in seconds and if ω_i is the injection frequency in radians per second, the Fourier coefficient of order 1 is

$$a_1 = (2/\pi) \int_0^{\pi} g'' \cos(\omega_i t) \, d(\omega_i t), \qquad (1)$$

where g" represents either g or g'. Now if θ_1 and θ_2 are the angular limits of $\omega_i t$ corresponding to the interval of potential or time being considered, and if this interval is quite small, and has been assumed, the variation of cos $(\omega_i t)$ over this interval is small enough so that $\omega_i t$ may be treated simply as a constant

β, where β is some angle between θ_1 and θ_2. Now (1) can be rewritten as an approximation

$$a_1 = \frac{2 \cos \beta}{\pi} \int_{\theta_1}^{\theta_2} g'' \, d(\omega_i t). \qquad (2)$$

The integral in (2) is simply the area under g or g' when plotted against time, and since these areas have been made approximately equal, we conclude that this integral has approximately the same value for g' as for g . Its value can be obtained from the g' curve by choosing the angular limits θ_1 and θ_2 to be the exact limits of the nonzero segment of g', as indicated in Fig. 2. The value of β is the same for both g' and g because of the equal center of gravity condition. Thus a_1 is the same for both g' and g. A similar analysis justifies the equal area conditions for i' and i.

III. CONVERSION TRANSCONDUCTANCE

It has been noted previously that when the load resistance R is not small a distinction may be made between the incremental transfer conductance g (or g') of the circuit as a whole, acting as a straight amplifier, and the incremental transconductance g_m of the tube alone. For the same condition, a distinction may be made between what might be called the conversion transfer conductance of the whole circuit as a heterodyne mixer and the conversion transconductance of the mixer tube alone. However, for simplicity, this distinction will be avoided here, and the symbol G_c will be used to represent both quantities.

Consider a mixer circuit whose characteristics are represented by the g' curve in Fig. 1. The development of the conversion transconductance G_c follows the familiar pattern, with a few exceptions. For the reader's convenience, we review it here. Suppose that a signal potential

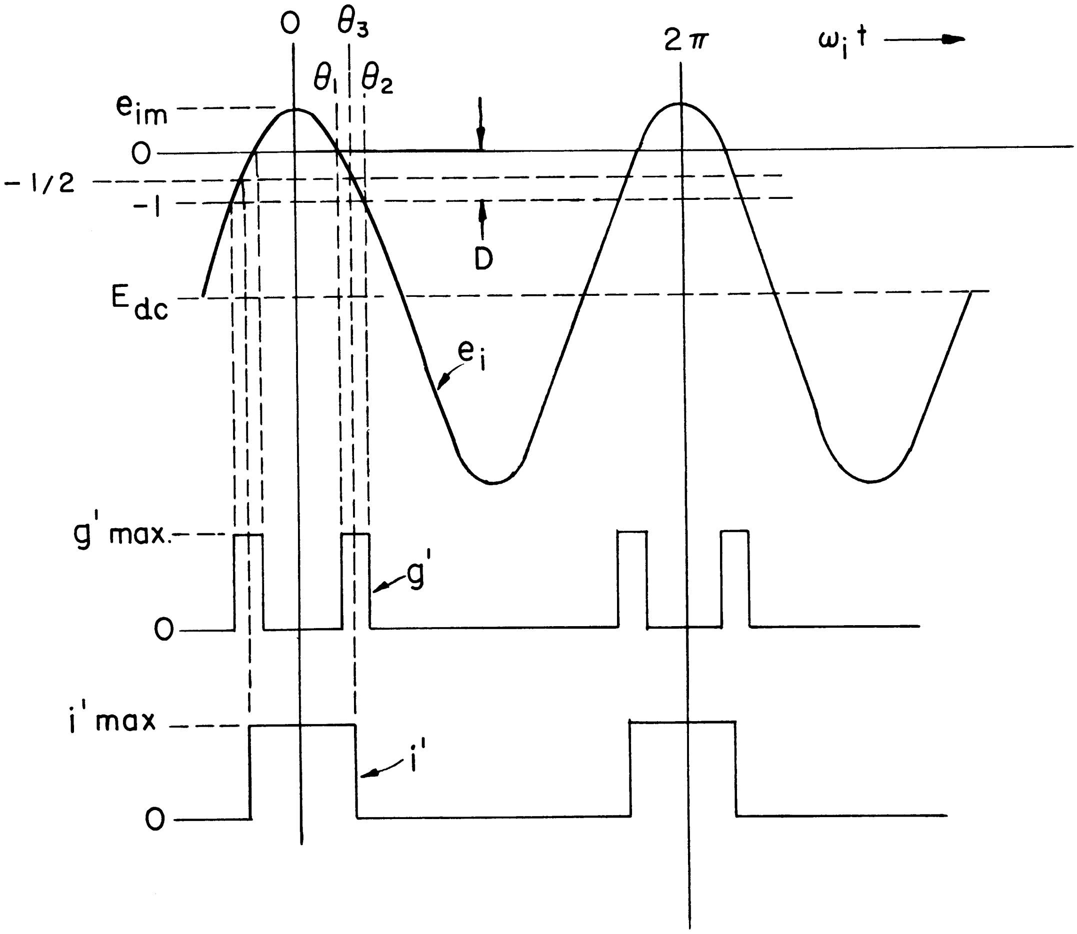

FIG. 2. RELATION BETWEEN INSTANTANEOUS VALUES OF INJECTION POTENTIAL e_i, TRANSFER CONDUCTANCE g', AND OUTPUT CURRENT i' AS FUNCTIONS OF TIME WHEN THE PIECEWISE-LINEAR APPROXIMATIONS ARE USED.

$$e_s = E_s \cos(\omega_s t), \tag{3}$$

where E_s is very small, is applied to the appropriate mixer terminal-pair. Since the transfer conductance g' was defined previously as the partial derivative of the output current with respect to e_s, we have

$$i_o = \int g' \, de_s, \tag{4}$$

where i_o is the output current (not shown in Fig. 1) corresponding to g'. Since E_s is very small, g' is essentially independent of e_s, so that

$$i_o = g' \int de_s = C + g'e_s , \tag{5}$$

where C is the constant of integration. Now let the injection voltage be an even function

$$e_i = E_{dc} + E_i \cos(\omega_i t). \tag{6}$$

Then g' and e_i are related in time as shown in Fig. 2, and g' can be written as a Fourier cosine series

$$g' = b_o/2 + b_1 \cos(\omega_i t) + b_2 \cos(2\omega_i t) + \text{etc.} \tag{7}$$

If (3) and (7) are now substituted for g' in (5), the current becomes

$$\begin{aligned} i_o = C + (b_o/2)E_s \cos(\omega_s t) &+ (b_1/2)E_s \cos(\omega_s - \omega_i)t \\ &+ (b_1/2)E_s \cos(\omega_s + \omega_i)t \\ &+ (b_2/2)E_s \cos(\omega_s - 2\omega_i)t \\ &+ (b_2/2)E_s \cos(\omega_s + 2\omega_i)t \\ &+ \text{etc.} \end{aligned} \tag{9}$$

One of the terms in (9) has an angular frequency $(\omega_s - \omega_i)$; the ratio of the coefficient of this term to the amplitude E_s of the signal potential is defined as the conversion transconductance G_c. Evidently,

$$G_c = b_1/2 \quad , \tag{10}$$

which is the well known relationship. The value of b_1 for the piecewise-linear function g' is given by the formula for the Fourier coefficient of an even function

$$b_1 = (2/\pi) \int_0^{\pi} g' \cos(\omega_i t)\, d(\omega_i t). \qquad (11)$$

From Fig. 1 or Fig. 2, it is seen that g' is equal to a constant maximum value g'_{max} over the dynamic interval and equal to zero elsewhere, so that if Θ_1 and Θ_2 are the angular limits of the g' pulse, as indicated in Fig. 2,

$$b_1 = (2/\pi) \int_{\Theta_1}^{\Theta_2} g'_{max} \cos(\omega_i t)\, d(\omega_i t). \qquad (12)$$

By substituting (12) in place of b_1 in (10) and performing the indicated integration, we obtain the following expression for the conversion transconductance G_c:

$$G_c = (g'_{max}/\pi)(\sin \Theta_2 - \sin \Theta_1) \qquad (13)$$

The difference $(\sin \Theta_2 - \sin \Theta_1)$ can vary from zero to unity, so that it can serve conveniently as a definition of the relative conversion transconductance, which will be denoted here by the symbol G_{crel}. Since Θ_1 and Θ_2 are quantities not easily measured, it is more useful to have G_{crel} expressed in terms of more easily measured quantities such as certain components of the injection potential. Three component values suggest themselves as possibilities: the d-c or bias component E_{dc}, the peak value E_{im} of the a-c component, and the peak instantaneous value e_{im} of the total injection potential (see Fig. 2). If two of these are known, the third is determined, so that only two are needed in the expression for G_{rel}. It happens that G_{crel} is most sensitive to changes in e_{im}, so that it seems logical to use e_{im} as one of the values in the new expression. E_{im} and E_{dc} are in general rather large quantities, while e_{im} is the small difference between them, so that if E_{im} and E_{dc} are taken as the measured values, a small fractional error in either results in a large fractional error in e_{im}. Consequently it is desirable to use e_{im} together with either one of the other two in the new expression for G_{crel}. E_{dc} has been chosen here. From trigonometry, we find that

$$G_{crel} = \sqrt{1 - \left(\frac{-E_{dc} - 1}{-E_{dc} + e_{im}}\right)^2} - \sqrt{1 - \left(\frac{-E_{dc}}{-E_{dc} + e_{im}}\right)^2} \quad (14)$$

while the last term can be dropped when e_{im} lies between zero and minus one, so that

$$G_{crel} = \sqrt{1 - \left(\frac{-E_{dc} - 1}{-E_{dc} + e_{im}}\right)^2} \quad (15)$$

Values of G_{crel}, as given by (14) and (15) and expressed in decibels, are plotted in Fig. 3 for the more interesting ranges of values. For comparison, Fig. 10 shows some measured values of G_{crel} taken from an experimental circuit which will be described subsequently. The comparison shows good agreement between theoretical and practical results when $(-E_{dc})$ is large and e_{im} is positive, as should be expected from the discussion in connection with (2).

It is interesting to note that when $(-E_{dc})$ is large in comparison with both e_{im} and unity the relative conversion transconductance becomes approximately equal to $\sqrt{2/(-E_{dc})}$, which suggests that the circuit might be useful as an analog for an inverse square root function. In any practical circuit, where the transconductance is more accurately described by g than by g' (Fig. 1), it would be necessary to hold e_{im} constant at zero or some small value in order to achieve this result.

IV. INJECTION FREQUENCY COMPONENT

Consider again the hypothetical mixer whose characteristics are represented by the curves in Fig. 1. Let the piecewise-linear approximation i' replace i in the analysis. (Note that i' is not the same as the i_o of the preceding section, which was obtained by integrating g' with respect to e_s.) As shown in Fig. 2, i' is an even function of time, so that it can be represented

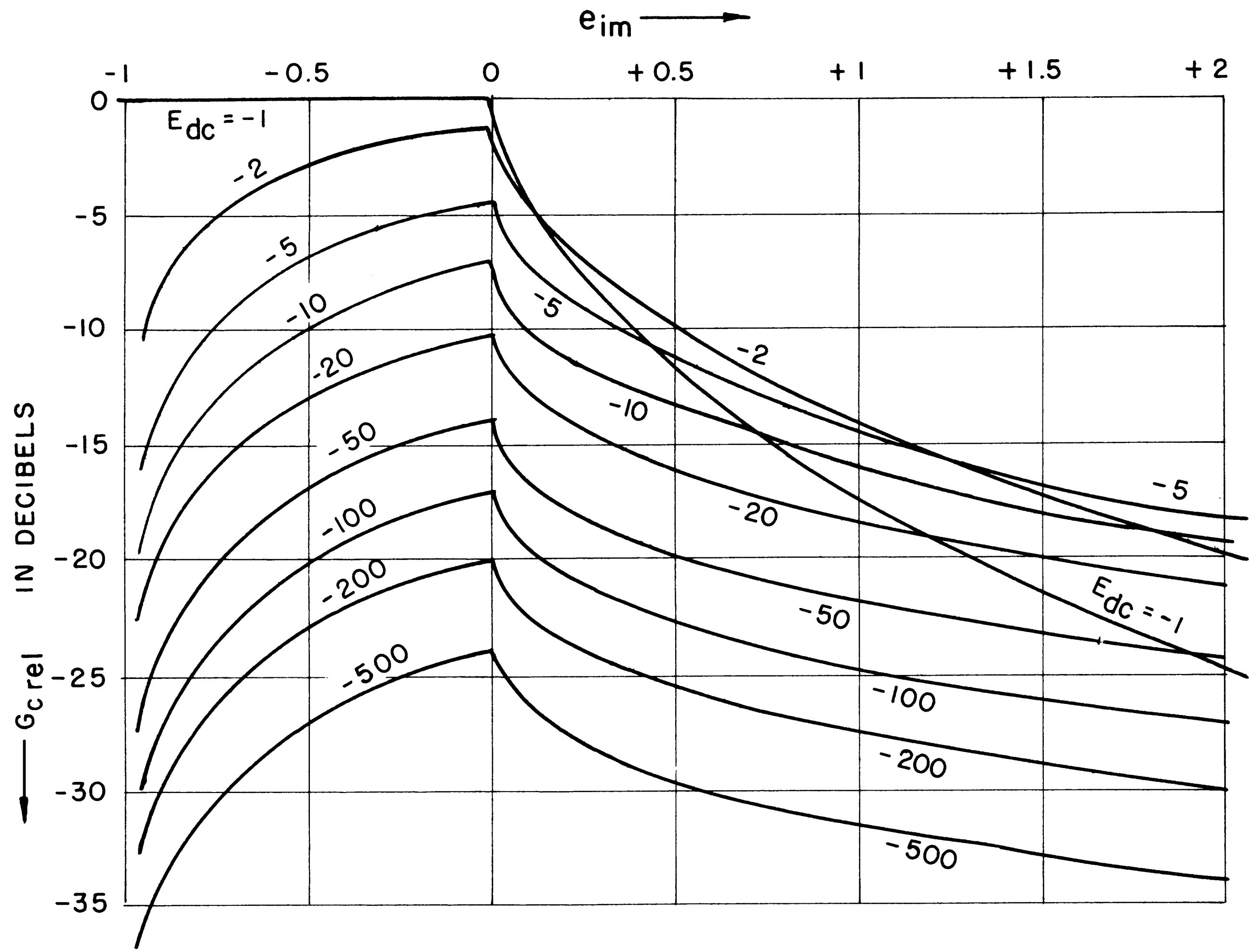

FIG. 3. THEORETICAL VALUES OF RELATIVE CONVERSION TRANSCONDUCTANCE G_{crel} OBTAINED FROM EQUATIONS (14) AND (15) EXPRESSED IN DECIBELS. THE SYMBOL E_{dc} REPRESENTS THE d-c INJECTION BIAS POTENTIAL AND e_{im} IS THE INSTANTANEOUS MAXIMUM TOTAL INJECTION POTENTIAL.

by a Fourier cosine series:

$$i' = B_0/2 + B_1 \cos(\omega_i t) + B_2 \cos(2\omega_i t) + \text{etc.} \tag{16}$$

The coefficient B_1 is evidently the amplitude of the injection-frequency component of the output current, and will hereafter be denoted as I_i. From the formula for the Fourier coefficient of an even function, we have

$$I_i = (2/\pi) \int_0^{\pi} i' \cos(\omega_i t)\, d(\omega_i t) \tag{17}$$

Let Θ_3 denote the value of $\omega_i t$ for which $e_i = -1/2$. It is evident from Fig. 2 that i' has a constant maximum value i'_{max} between 0 and Θ_3 and a value of zero between Θ_3 and π so that (17) may be rewritten as

$$I_i = (2/\pi)\, i'_{max} \int_0^{\Theta_3} \cos(\omega_i t)\, d(\omega_i t) = (2/\pi)\, i'_{max} \sin \Theta_3 \tag{18}$$

As a function of Θ_3, I_i evidently has a maximum value equal to $(2/\pi) i'_{max}$ when $\Theta_3 = \pi/2$ and a relative value

$$I_{irel} = \sin \Theta_3 . \tag{19}$$

From trigonometry, I_{irel} can be evaluated in terms of E_{dc} and e_{im} as

$$I_{irel} = \sqrt{1 - \left(\frac{-E_{dc} - 1/2}{-E_{dc} + e_{im}} \right)^2} \tag{20}$$

Values of (20), expressed in decibels, are plotted in Fig. 4 as functions of e_{im}, with E_{dc} as a parameter.

By dividing either (14) or (15) by (20), depending upon the value of e_{im}, we obtain a number which is proportional to the ratio of the amplitude of the desired difference-frequency component to the amplitude of the undesired injection-frequency component in the output current. Since this number is only proportional to, not equal to, the ratio of the amplitudes, its actual value is of less interest than the way in which its value changes with e_{im} for different

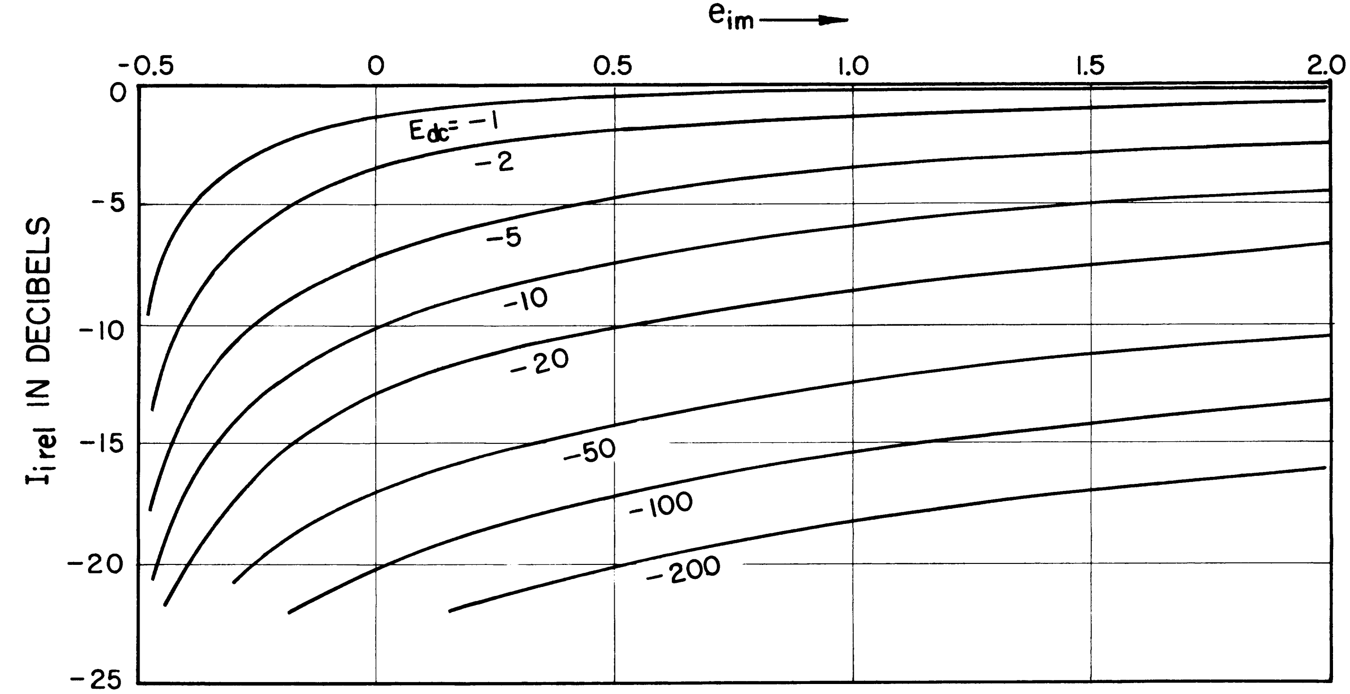

FIG. 4. GRAPH OF THE RELATIVE AMPLITUDE $I_{i\,rel}$ OF THE INJECTION-FREQUENCY COMPONENT IN THE OUTPUT CURRENT, ACCORDING TO EQUATION (20), EXPRESSED IN DECIBELS.

2262 A-G8-72 RRC 10-28-55

values of E_{dc}. This is shown in Fig. 5, where ordinates are expressed in decibels. The curves of Fig. 5 may be obtained simply by subtracting the curves of Fig. 4 from those of Fig. 3, for the corresponding values of E_{dc}. In the limiting case where E_{dc} approaches minus infinity,

$$\frac{G_{crel}}{I_{irel}} = \frac{\sin \theta_2 - \sin \theta_1}{\sin \theta_3} = \sqrt{\frac{2(e_{im} + 1)}{2e_{im} + 1}} - \sqrt{\frac{2e_{im}}{2e_{im} + 1}} \qquad (21)$$

for the case where e_{im} is positive and

$$\frac{G_{crel}}{I_{irel}} = \frac{\sin \theta_2 - \sin \theta_1}{\sin \theta_3} = \sqrt{\frac{2(e_{im} + 1)}{2e_{im}+1}} \qquad (22)$$

for the case where e_{im} lies between -1/2 and zero. These are relative values. The actual value of the ratio of the amplitude of the difference-frequency component of the output current to the amplitude of the injection-frequency component of the same current can be obtained, in decibels, by adding the term $20 \log_{10} (E_s g'_{max}/2i'_{max})$ to the curves of Fig. 5. Here, E_s is the peak amplitude of the signal potential, as indicated by (3), and g'_{max} and i'_{max} are the values used in (12) and(18) and pictured graphically in Fig. 2. This ratio is important in cases where the injection frequency and difference frequency are not widely separated, since the filter which usually follows the mixer must be designed to pass one and rejct the other.

The curves of Fig. 5 exhibit sharp corners at $e_{im} = 0$ and steep slopes as e_{im} approaches -1/2 because of the discontinuities in the i' and g' curves at these points. In curves representing measurements in actual circuits, these features are missing, as would be expected. Figure 12, for example, shows curves of measured values in a particular circuit to be described subsequently.

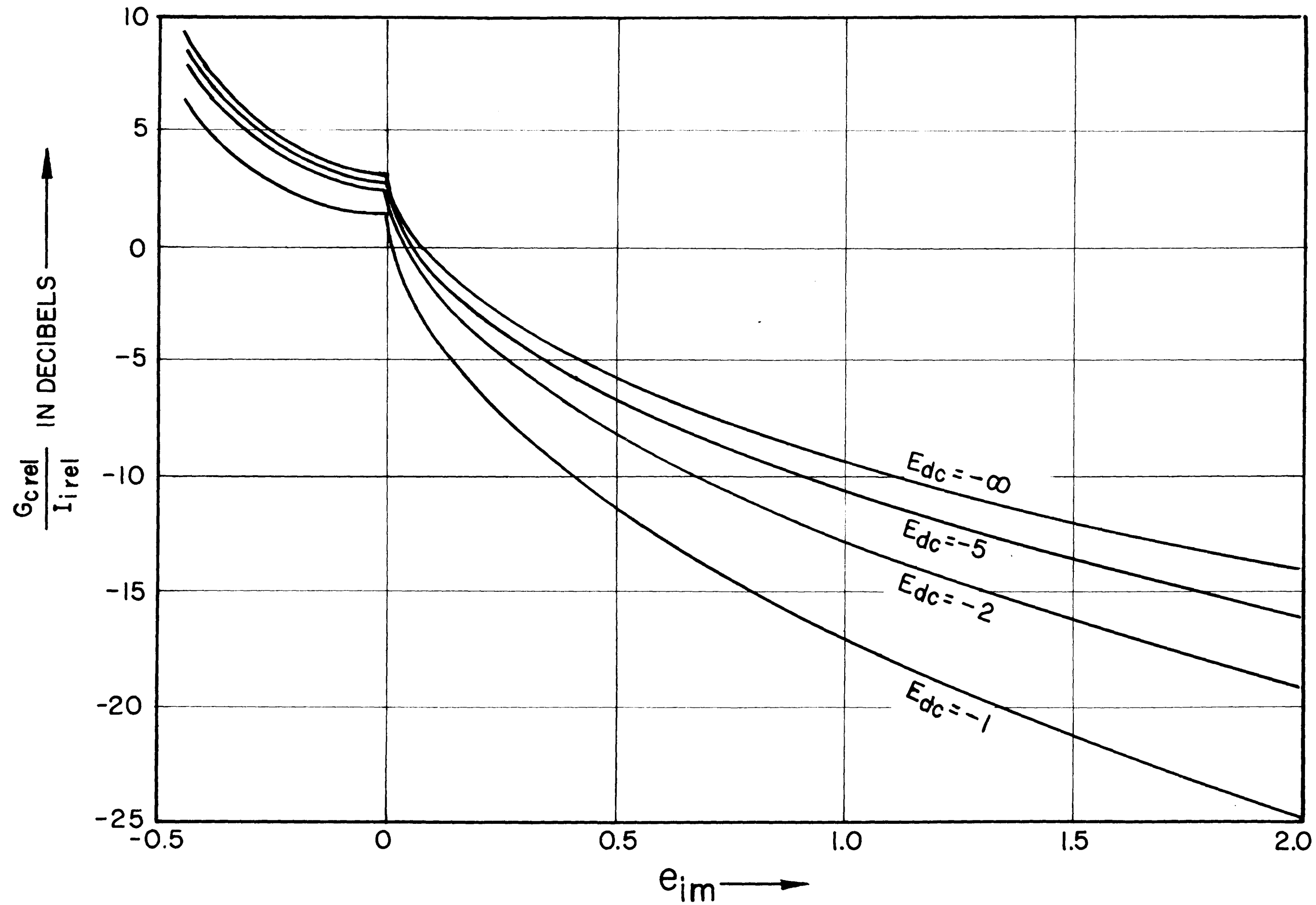

FIG. 5. GRAPH OF THE RATIO OF THE RELATIVE CONVERSION TRANSCONDUCTANCE $G_{c\,rel}$ TO THE RELATIVE AMPLITUDE $I_{i\,rel.}$ OF THE INJECTION-FREQUENCY COMPONENT IN THE OUTPUT CURRENT, ACCORDING TO EQUATIONS (14), (15), AND (20), EXPRESSED IN DECIBELS. THE LIMITING CASE, WHERE $E_{dc}=-\infty$, IS GIVEN BY EQUATIONS (21)

The theoretical and measured curves show reasonably close agreement, however, for values of e_{im} well removed from -0.5 and 0.

V. INJECTION MODULATION COMPONENT

The injection source always has a slight modulation in its amplitude because of noise, power-frequency ripple, microphonics, etc. When the injection potential in a heterodyne mixer becomes very large, these variations become important. The d-c component I_{dc} of the output current of the mixer is a function of the amplitude of the injection potential. Consequently, when the injection potential varies in amplitude in accordance with noise, ripple, or microphonics, the d-c output current varies in a corresponding manner. The variation in injection potential amplitude is equivalent to an equal variation in the peak value e_{im} while E_{dc} remains constant. Consequently, the relative amplitude of the injection modulation-frequency component in the output current can be expressed in terms of the slope of a curve of the d-c current plotted against e_{im}, for various fixed values of E_{dc}.

In Eq (16), the d-c component of i' is $I_{dc} = B_0/2$. The formula for this Fourier coefficient is

$$I_{dc} = B_0/2 = (1/\pi) \int_0^{\pi} i' \, d(\omega_i t) \qquad (23)$$

From inspection of Fig. 2, it is evident that i' is equal to a constant value i'_{max} between the limits $\omega_i t = 0$ and $\omega_i t = \theta_3$, and equal to zero from $\omega_i t = \theta_3$ to $\omega_i t = \pi$, so that (23) reduces to

$$I_{dc} = B_0/2 = (1/\pi) \int_0^{\theta_3} i'_{max} \, d(\omega_i t) = (\theta_3/\pi) \, i'_{max} \qquad (24)$$

In general, E_{dc} is a large negative quantity. For the present, it is assumed that

E_{dc} is at least as negative as -1/2. For this limiting case, $\theta_3 = \pi/2$, so that the corresponding limiting value of $B_0/2$ is $(I_{dc})_{max} = (1/2)i'_{max}$. The relative value $(I_{dc})_{rel}$ of the d-c current component I_{dc} is therefore equal to

$$(I_{dc})_{rel} = \frac{I_{dc}}{(I_{dc})_{max}} = \frac{I_{dc}}{(1/2)i'_{max}} = \frac{\theta_3}{\pi/2} \tag{25}$$

A graph of this quantity is given in Fig. 6 as a function of e_{im}, with E_{dc} as a parameter.

It is evident in Fig. 6 that all curves approach zero very rapidly as e_{im} approaches -1/2, where Fig. 1 shows a discontinuity in i'. This would lead to the conclusion that the injection modulation component, which is proportional to the slope of the curves, as mentioned above, should have a very large value as e_{im} approaches -1/2. However, in any practical circuit, a sharp discontinuity in i' such as that shown by the dashed line in Fig. 1 does not occur; the actual behavior is more like that represented by the solid line in the same figure. Consequently, steep slopes in the d-c curves are absent in practice, and the curves of Fig. 6 are not particularly useful for negative values of e_{im}. For example, Fig. 11 shows some relative d-c current values measured in a mixer circuit which will be described subsequently. It can be seen that the agreement between these measured characteristics and the curves of Fig. 6 is quite good for positive values of e_{im}. Many mixers are operated with e_{im} in this positive region, so that for many practical situations equation (25) and Fig. 6 are quite satisfactory.

From elementary trigonometry, we find that the angle θ_3 is (25) is

$$\theta_3 = \text{arcsec} \frac{-E_{dc} + e_{im}}{-E_{dc} - 1/2} \tag{26}$$

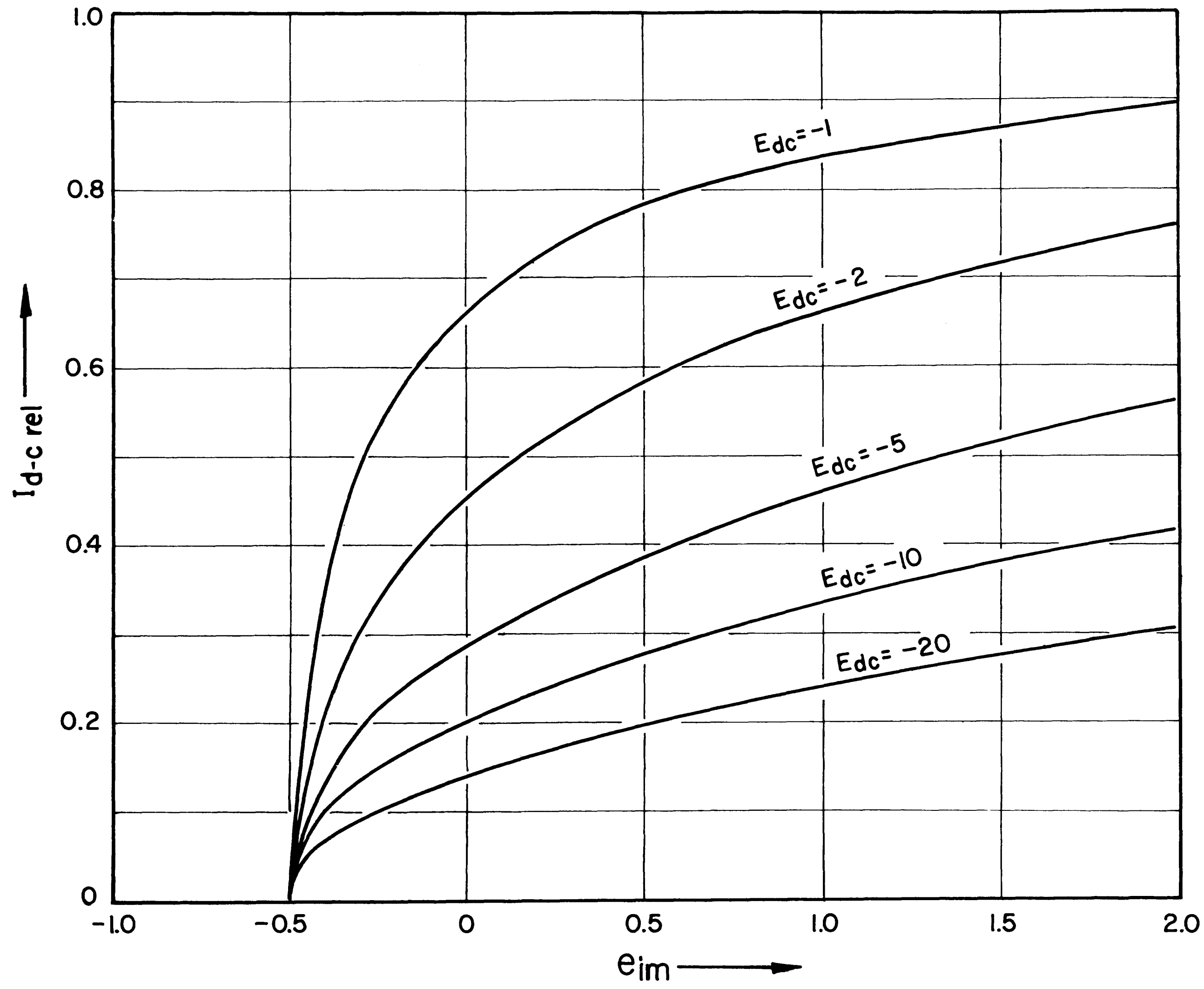

FIG. 6. GRAPH OF THE RELATIVE VALUE $I_{dc\ rel}$ OF THE D-C COMPONENT OF THE OUTPUT CURRENT, ACCORDING TO EQUATION (25). ALL CURVES APPROACH UNITY AS e_{im} BECOMES VERY LARGE.

2262 A-G8-74 RRC 10-28-55

The derivative of (26) with respect to e_{im} is

$$\frac{d}{de_{im}} \theta_3 = \frac{(-E_{dc} - 1/2)}{(-E_{dc} + e_{im})\sqrt{(-E_{dc} + e_{im})^2 - (-E_{dc} - 1/2)^2}} , \qquad (27)$$

which is a measure of the relative amplitude of the injection modulation-frequency component. The ratio of the relative conversion transconductance as given by (14) and (15) to the relative amplitude of the injection modulation-frequency component given by (27) is a figure of merit for the mixer which is worth some attention when the injection modulation component falls within the passband of the difference-frequency filter following the mixer. The symbol α will be used here to represent this ratio. When e_{im} lies between -1/2 and 0, α is found by dividing (15) by (27), with the following result:

$$\alpha = \frac{\sqrt{e_{im}^2 - 2E_{dc}e_{im} - 2E_{dc} - 1}\ \sqrt{e_{im}^2 - 2E_{dc}e_{im} - E_{dc} - 1/4}}{(-E_{dc} - 1/2)} \qquad (28)$$

When e_{im} is positive, α is found by dividing (14) by (27), with the result

$$\alpha = \frac{\left[\sqrt{e_{im}^2 - 2E_{dc}e_{im} - 2E_{dc} - 1} - \sqrt{e_{im}^2 - 2E_{dc}e_{im}}\right]\sqrt{e_{im}^2 - 2E_{dc}e_{im} - E_{dc} - 1/4}}{(-E_{dc} - 1/2)} \qquad (29)$$

The value of α, expressed in decibels, is plotted in Fig. 7 as a function of e_{im}, with E_{dc} as a parameter. The value evidently changes very little as a function of E_{dc}, so that only three curves, drawn for E_{dc} = -1, -2, and - ∞, are sufficient to describe it. In the limiting case where $E_{dc} = -\infty$, (28) and (29) reduce, respectively, to

$$\alpha = \sqrt{2(e_{im} + 1)\ (2e_{im} + 1)} \qquad (30)$$

and

$$\alpha = \left(\sqrt{2(e_{im} + 1)} - \sqrt{2e_{im}}\right)\sqrt{2e_{im} + 1} \qquad (31)$$

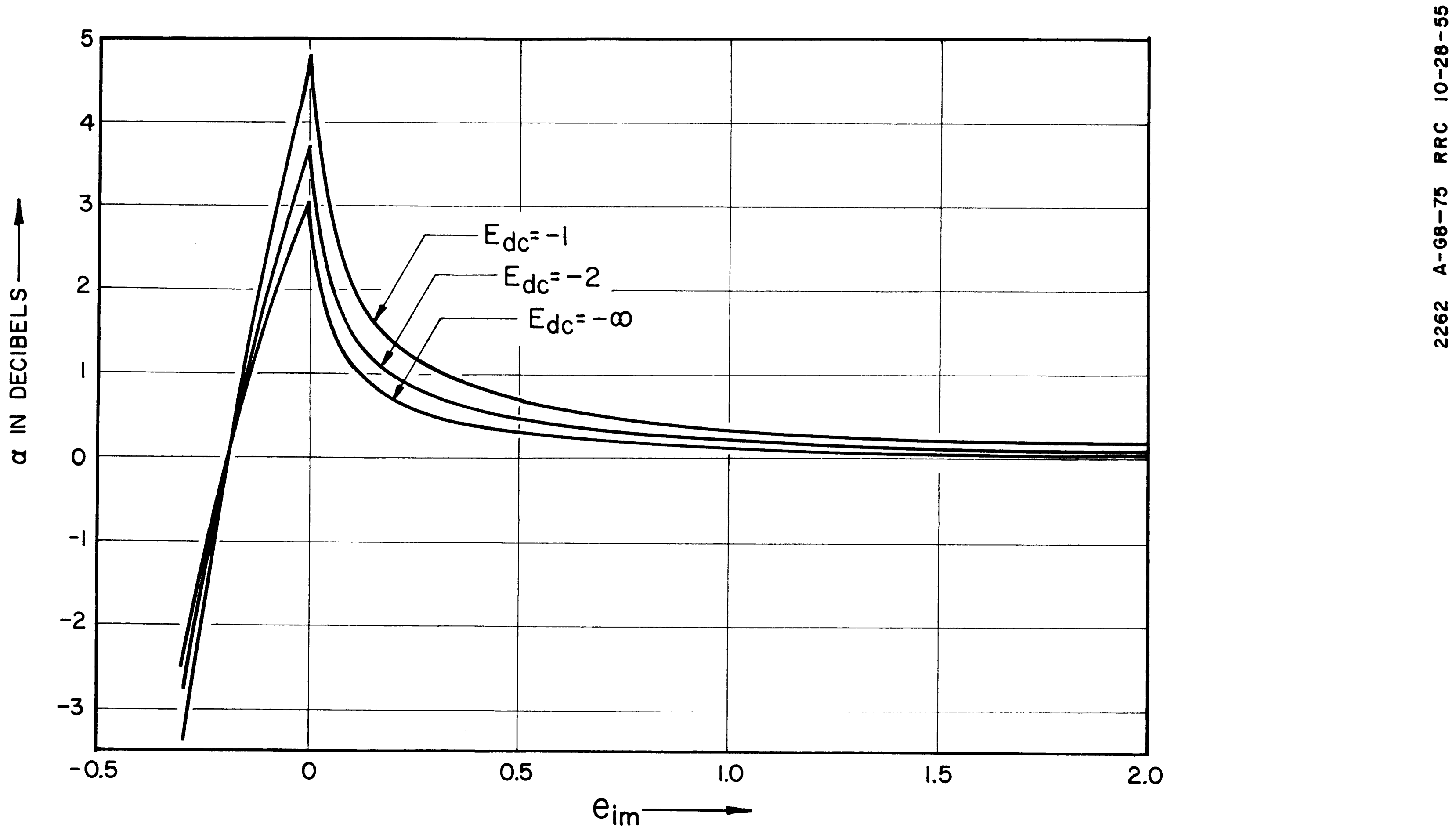

FIG. 7. THEORETICAL VALUE OF THE FIGURE OF MERIT α, DEFINED BY EQUATIONS (28), (29), (30), AND (31), EXPRESSED IN DECIBELS.

The sharp points in the curves at $e_{im} = 0$ are due to the discontinuity in g' at this point, while the large attenuation as e_{im} approaches -1/2 is due to the discontinuity in i', as mentioned previously. In a practical circuit, the sharp points are rounded off and the attenuation is less severe.

All of the curves in Fig. 7 approach zero as e_{im} becomes more positive. Evidently the conversion transconductance and the injection modulation component both decrease at the same rate as e_{im} becomes large, so that nothing is to be gained or lost as far as α is concerned by changing from one large positive value of e_{im} to another.

VI. EXPERIMENTAL RESULTS

As an illustration of the piecewise-linear method of mixer analysis, the experimental circuit shown in Fig. 8 is used. The signal and injection frequencies are 1000 and 60 cycles per second, respectively. The output current through the 24,000 ohm resistor R_3, is proportional to the output potential, the components of which are measured by means of a high-resistance d-c voltmeter and a high-impedance audio-frequency wave-analyzer. The measured values of the d-c output voltage and the relative transconductance are plotted as solid lines in Fig. 9, as functions of the measured d-c component of the input potential.
The dashed lines in Fig. 9 are piecewise-linear approximations determined in the manner described in connection with Fig. 1, with which Fig. 9 may be compared. For convenience in relating the measured values to the theoretical values, the 1.5 volt cell E_1 and the potentiometer R_1 are included in the input circuit and the potentiometer is adjusted to make the right-hand step in g' fall at exactly zero volt on the e_i scale. The cell E_2 and the potentiometer R_4 in the output circuit are used to adjust the d-c level of the output potential to the desired position.

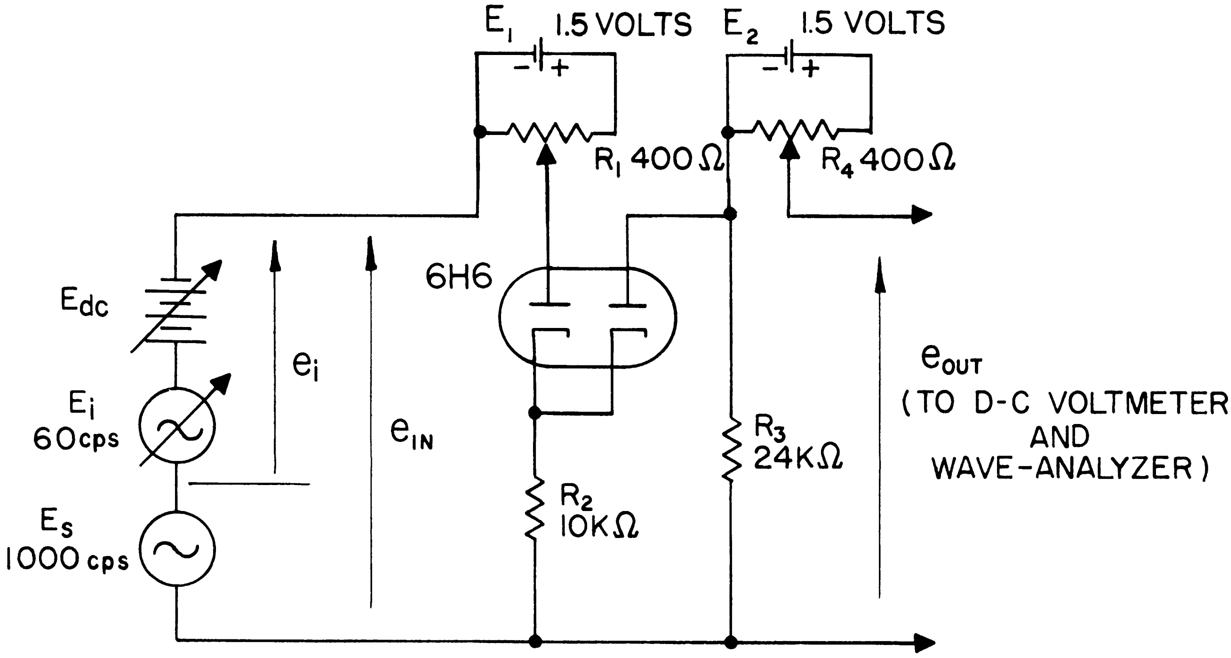

FIG. 8. AN EXPERIMENTAL CIRCUIT USED TO ILLUSTRATE THE APPLICATION OF THE PIECEWISE-LINEAR ANALYSIS.

2262 A-G8-102 BM 2-28-56

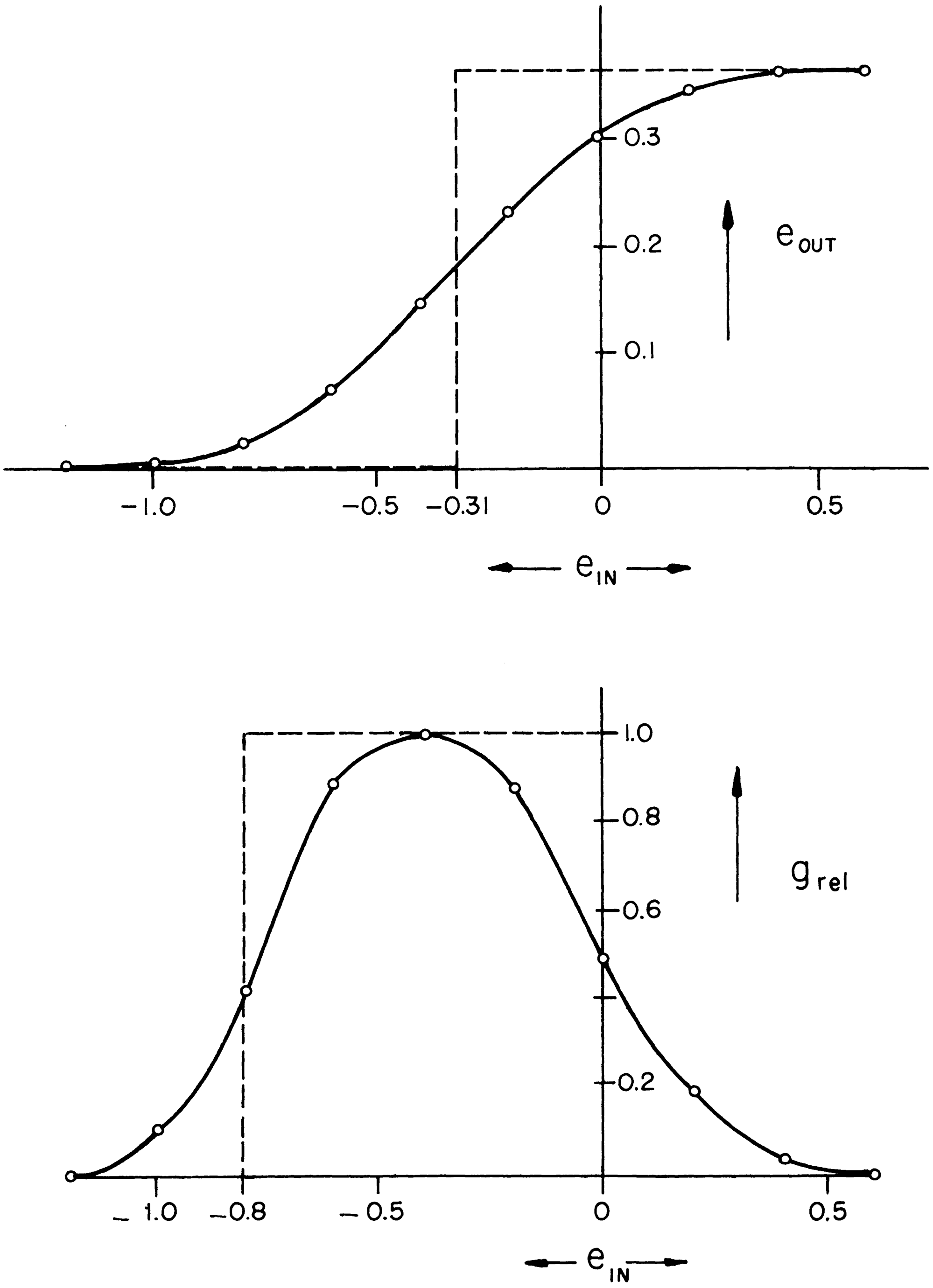

FIG. 9. MEASURED VALUES OF INSTANTANEOUS OUTPUT POTENTIAL e_{OUT} AND INCREMENTAL TRANSFER CONDUCTANCE g IN THE CIRCUIT OF FIG. 8, AS FUNCTIONS OF INSTANTANEOUS TOTAL INJECTION POTENTIAL e_i.

By applying a graphical integration method to the g curve, the proper dynamic range of the g' curve is found to be 0.8 volt. This value then serves as the basis of normalization for the input voltage components E_{dc} and e_{im} where they appear in Figs. 10, 11, and 12, so that these graphs of the measured values can be compared directly with the theoretical curves in Figs. 3, 5, and 6. In Fig. 9, the abscissa represents the actual measured input potential, not the normalized value. When R_1 is adjusted so that the right-hand step in g' falls exactly at zero, the left-hand step then falls at -0.8 volt (normalized value -1). Another graphical integration, this time applied to the i curve, then establishes the correct location for the step in i' at -0.31 volt (normalized value about -0.39).

Relative values of conversion transconductance for the circuit of Fig. 8 are measured directly with the audio-frequency wave-analyzer. The results are plotted in Fig. 10. There is good agreement between these curves and the theoretical curves of Fig. 3, especially for large values of $-E_{dc}$ and $+e_{im}$. The sharp corners in Fig. 3 are rounded off in Fig. 10, and the rapid decrease as e_{im} approaches -1 is less pronounced in the actual circuit, as is to be expected.

Relative values of measured d-c output potential (or current) are plotted in Fig. 11. These curves compare quite well with the theoretical curves of Fig. 6 for positive values of e_{im}, but, as expected, not well for negative values. As mentioned previously, however, many mixers operate with positive values of e_{im}.

Figure 14 shows the ratio of the measured values of G_{crel} and I_{irel} for the circuit of Fig. 8, expressed in decibels. These curves compare favorably with the theoretical values plotted in Fig. 5, except for values of e_{im} near

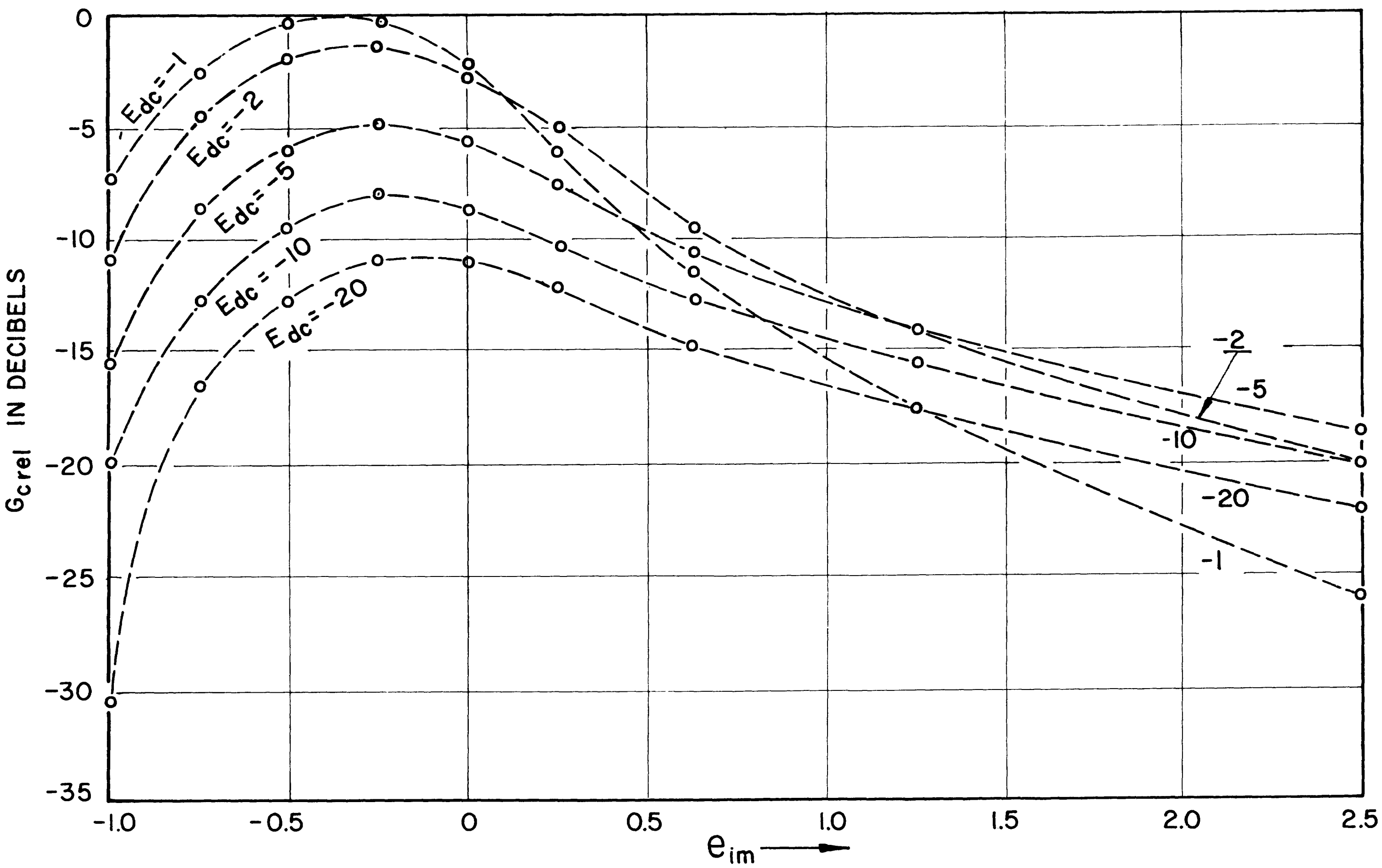

FIG. 10. MEASURED VALUE OF RELATIVE CONVERSION TRANSCONDUCTANCE IN THE CIRCUIT OF FIGURE 8. THIS MAY BE COMPARED WITH THE THEORETICAL VALUES OF FIGURE 3.

2262 A-G8-77 RRC 10-27-55

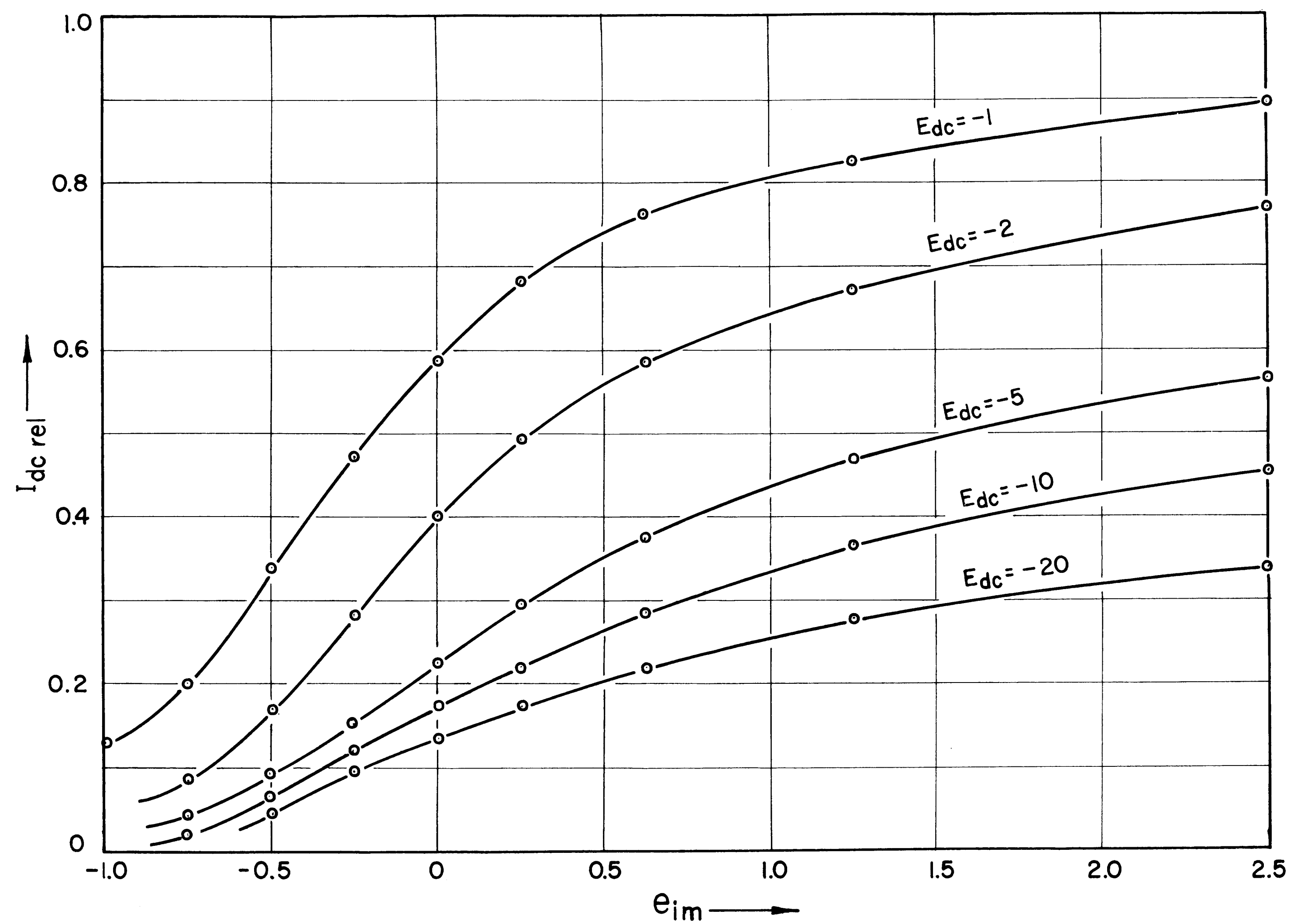

FIG. 11. EXPERIMENTAL MEASUREMENTS OF RELATIVE D-C CURRENT IN THE OUTPUT OF THE CIRCUIT OF FIGURE 8. THESE CURVES MAY BE COMPARED WITH THE THEORETICAL CURVES IN FIGURE 6.

2262 A-G8-78 RRC 10-27-55

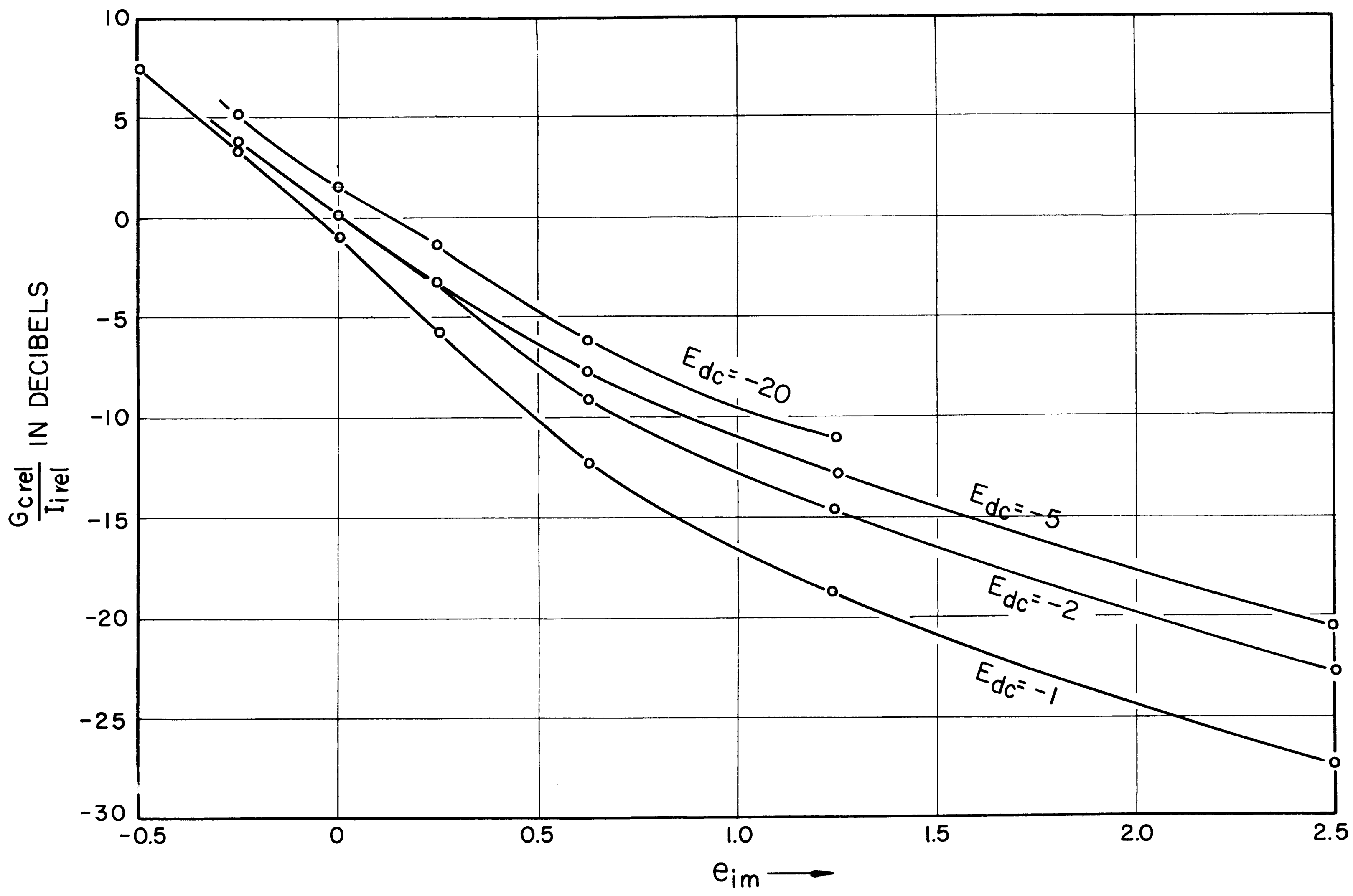

FIG. 12. THE RATIO OF THE MEASURED VALUES OF $G_{c\,rel}$ AND $I_{i\,rel}$ FOR THE CIRCUIT OF FIGURE 8, EXPRESSED IN DECIBELS. THESE CURVES MAY BE COMPARED WITH THE THEORETICAL CURVES OF FIGURE 5.

2262 A-G8-79 RRC 10-28-55

0 or -0.5, as mentioned previously in connection with the discussion of Equations (20), (21), and (22) and Figure 5.

DISTRIBUTION LIST

1 Copy	Director, Electronic Research Laboratory Stanford University Stanford, California Attn: Dean Fred Terman
1 Copy	Commanding General Army Electronic Proving Ground Fort Huachuca, Arizona Attn: Director, Electronic Warfare Department
1 Copy	Chief, Research and Development Division Office of the Chief Signal Officer Department of the Army Washington 25, D. C. Attn: SIGEB
1 Copy	Chief, Plans and Operations Division Office of the Chief Signal Officer Washington 25, D. C. Attn: SIGEW
1 Copy	Countermeasures Laboratory Gilfillan Brothers, Inc. 1815 Venice Blvd. Los Angeles 6, California
1 Copy	Commanding Officer White Sands Signal Corps Agency White Sands Proving Ground Las Cruces, New Mexico Attn: SIGWS-CM
1 Copy	Commanding Officer Signal Corps Electronics Research Unit 9560th TSU Mountain View, California
60 Copies	Transportation Officer, SCEL Evans Signal Laboratory Building No. 42, Belmar, New Jersey FOR - SCEL Accountable Officer Inspect at Destination File No. 22824-PH-54-91(1701)

1 Copy	H. W. Welch, Jr. Engineering Research Institu University of Michigan Ann Arbor, Michigan
1 Copy	J. A. Boyd Engineering Research Institute University of Michigan Ann Arbor, Michigan
1 Copy	Document Room Willow Run Research Center University of Michigan Willow Run, Michigan
11 Copies	Electronic Defense Group Project File University of Michigan Ann Arbor, Michigan
1 Copy	Engineering Research Institute Project File University of Michigan Ann Arbor, Michigan